

## CONTROL OF TORSION EFFECTS IN BUILDINGS WITH EXTREME TORSIONAL IRREGULARITY THROUGH THE USE OF HYSTERETIC HEATSINKS-SLB

### KONTROLA TORZIONIH EFEKATA U ZGRADAMA SA EKSTREMNOM TORZIONOM NEPRAVILNOŠĆU KORIŠĆENJEM HISTEREZISNIH DISIPATORA-SLB



Originalni naučni rad / Original scientific paper


Rad primljen / Paper received: 15.12.2022

<https://doi.org/10.69644/ivk-2024-03-0360>

Adresa autora / Author's address:

The Pontifical Catholic University of Peru

I.J.R. Manoslava  0000-0002-2893-7351; J.G.V. Alayo 

0000-0002-5772-6879; J.A.A. Martinez  0000-0003-4154-9510;

\*email: [a20194397@pucp.edu.pe](mailto:a20194397@pucp.edu.pe)

#### Keywords

- seismic analysis
- torsional irregularity
- time-history analysis

#### Abstract

*Torsional irregularities are one of the main causes of failure in structures during seismic events, which must be considered because they can cause them to collapse. This type of irregularity is included in many seismic codes in the world. In this study, the behaviour of a 7-story building is evaluated, for which 2 types of analyses are carried out separately, one of the methods is defined by the Peruvian code-2018 (E.030-2018), and for the other it was proposed to incorporate a seismic protection system, based on SLB hysteretic heatsinks, using a modal spectral analysis and nonlinear time history. Iterations were carried out to achieve the most effective location of the devices, thus strategically proposing 3 lines of resistance with SLB heatsinks. In this way, only at certain parts of the building that are provided with the use of the devices, will energy absorption and nonlinear behaviour occur. Results of the response history show that with the incorporation of heatsinks the damping is increased, and drifts of the floors are reduced by 60 % and displacements by 70 %. It is concluded that incorporation of these devices controls the effect of extreme torsional behaviour of the structure.*

#### INTRODUCTION

The most severe earthquakes leave great lessons. Over time, during strong seismic events it has been observed that structures with torsional irregularity can suffer serious damage, leading to their collapse /1/. This is because the centre of mass and the centre of rigidity are not in the same place. For this reason, an excessive increase in lateral movement occurs when dynamic loads excite buildings, becoming one of the most severe causes of vulnerabilities, /2/.

Current seismic codes, such as the European code EC-8, ASCE 7-16, Peruvian standard E.030-2018, among others, that ensure the performance of structures with torsional irregularity, incorporate special requirements that vary according to a series of factors that include the geometry of the plan, dimensions and positions of structural elements. and floor numbers /3/. In addition to a procedure based on the calculation through torque equations, and by changing the centre of mass to eliminate eccentricity, placing masses, or additional structural components on each floor.

#### Ključne reči

- seizmička analiza
- torziona nepravilnost
- vremensko-istorijska analiza

#### Izvod

*Torzione nepravilnosti su jedan od glavnih uzroka razaranja u konstrukcijama tokom seizmičkih događaja, što se mora uzeti u obzir jer mogu izazvati urušavanje. Ova vrsta nepravilnosti je sadržana u mnogim seizmičkim kodovima u svetu. U ovoj studiji se ocenjuje ponašanje zgrade od 7 spratova, gde je posebno obavljeno 2 tipa analiza, od kojih je jedna metoda definisana Peruanskim standardom-2018 (E. 030-2018), a kod druge je predložena ugradnja sistema seizmičke zaštite, zasnovan na SLB histerezisnim disipatorima, korišćenjem modalne spektralne analize i nelinearne vremenske istorije. Iteracije su sprovedene radi iznalaženja najefikasnije lokacije uređaja, čime su strateški predložene 3 linije otpora sa SLB elementima za odvođenje energije. Na ovaj način će samo u pojedinim delovima zgrade, koji su obezbeđeni uređajima, energija biti apsorbovana uz nelinearno ponašanje. Rezultati istorije odziva pokazuju da se ugradnjom disipatora prigušenje povećava, smaknutost spratova se smanjuje za 60 %, a pomeranje za 70 %. Zaključuje se da se ugradnjom ovih uređaja kontroliše efekat ekstremnog torzionog ponašanja konstrukcije.*

However, the lack of consensus between design regulations, and the results of recent earthquakes have shown that concrete structures with extreme torsion problems are very difficult and even impossible to repair. Such as the earthquake that occurred in the city of Pisco on August 15, 2007, of moment magnitude  $MW = 8.0$ , which left at least 519 dead. The damages were considerable which were magnified when the structures were also irregular, /4/.

This suggests the need to consider advantages of modern seismic design methods and incorporate energy dissipation systems to control the responses to the demands of a seismic event.

Current investigations such as *Procedure to optimize the structural design for buildings equipped with hysteretic SLB devices* by R. Chianese, conclude that these devices represent a good solution for seismic protection of buildings because they provide a significant contribution to the reduction of drift between floors and a great energy dissipation capacity due to its hysteretic behaviour /5/. In the article *Modeling, analysis and seismic design of structures using energy dissipation*

pators SLB, /6/, it is explained that these devices can dissipate the energy introduced by an earthquake in the structure, protecting other structural elements from being damaged /6/. Guillermo Bozzo proposes a new type of heatsink that manages to extend the deformation limits of current SLB devices and, in addition, meets similar requirements to those of restricted buckling arms in the AISC standard in terms of their cyclic load protocols and essays, /7/.

Many devices have been proposed in literature so far, characterised by different shapes, constituent material, and energy dissipation principle. However, the idea of using a passive control system, which does not need an external power source to work, and which, combined with reinforced concrete frames and uncoupled walls with heat sinks, increases rigidity and ductility /8/. It offers a viable alternative that in practical terms reduces possible structural damage by reducing design forces below the elastic limit.

Therefore, current research in order to improve the seismic response to extreme torsion problems and ensure its continued functionality, proposes the incorporation of Bozzo Shear Link heatsinks (SLB) into the structure.

## MATERIALS AND METHODS

Two types of structures are proposed, modelled and analysed using ETABS software (CSI 2018.1). These models include a 7-level structure, a type A and type B model. The heatsinks are incorporated in the type B.

As shown in Fig. 1, the type A model is observed, a 7-story building that presents a conventional structure made up of a dual system, structural walls, and reinforced concrete porticos. Where seismic response is evaluated by means of a spectral modal analysis presenting extreme torsional irregularity. If the coefficient of torsional irregularity, which determines the amount of torsion in the building, is greater than 1.5 in either direction, the building is assumed to have extreme torsional irregularity, /9/.

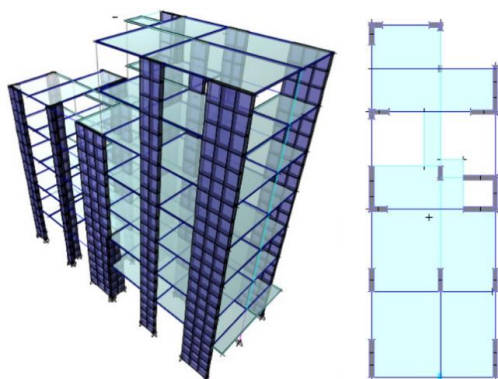


Figure 1. Type A model.

The second model is type B, in this model SLB heatsinks are incorporated to control extreme torsional irregularity. The locations of these devices are raised in 3 additional lines of resistance, these are lines of defence that represent structural redundancy that are resistant to lateral loads and that cause a high degree of hyperstaticity, /10/. Figure 2 shows the floors from the second to the fifth level, this level being a typical floor up to the seventh level, where these devices are located.

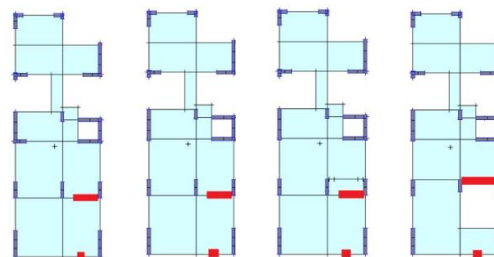


Figure 2. Type B model, floors from the second to the fifth level.

Figure 3a shows the 3D model in which 2 types of heat-sinks are represented: uncoupled walls and chevron diagonals considered at the level of the entire structure. Figure 3b shows the first line of resistance formed by chevron diagonals that go from the second to the seventh level on the façade. In Fig. 3c, 3 heatsinks are proposed on uncoupled walls that go from the second to the fifth level, and finally, in Fig. 3d, a third resistance line is added with 3 more heat-sinks on uncoupled walls, from the fifth to the seventh level.

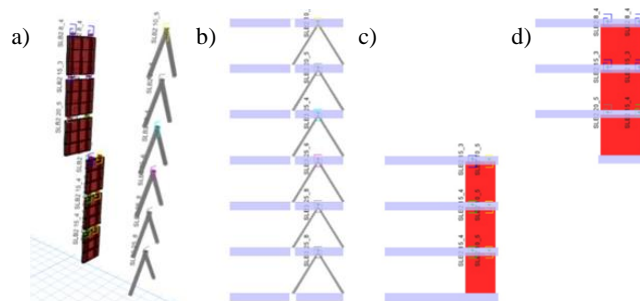


Figure 3. Elevation of SLB heatsinks, used in the type B model.

For the seismic analysis of the type B model, the modal overlap (MS) method and the nonlinear time history analysis (THNL) method were used. For the MS, a building importance factor of 1 and seismic zone 4 are considered. For the THNL analysis, two sets of ground acceleration records are used, each of which includes two components in orthogonal directions, /11/.

Pisco

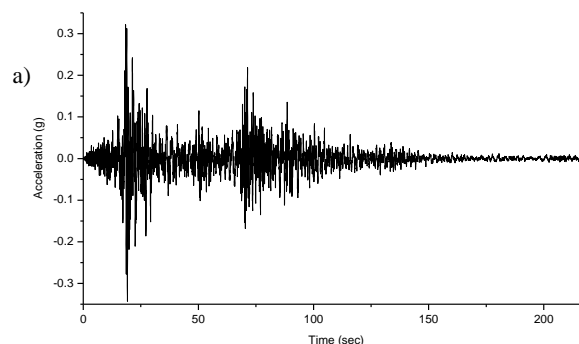
Earthquake of August 15, 2007 - EW component, ( $\Delta t = 0.01$  s and duration 218.06 s), 0.2771g (Fig. 4a).

Earthquake of August 15, 2007 - NS component, ( $\Delta t = 0.01$  s and duration 218.06 s), 0.3425g (Fig. 4b).

Moquegua

Earthquake of June 23, 2001 - EW component, ( $\Delta t = 0.01$  s and duration 198.91 s), 0.3014g (Fig. 5a).

Earthquake of June 23, 2001 - NS component, ( $\Delta t = 0.01$  s and duration 198.91 s), 0.2239g (Fig. 5b).



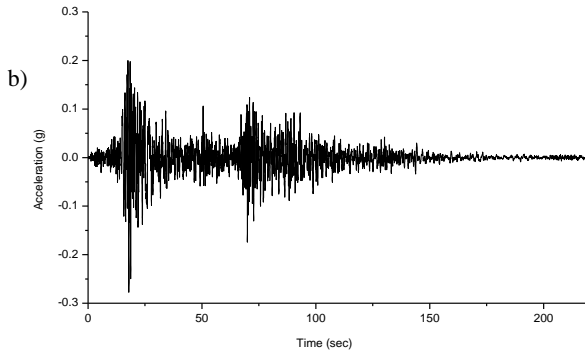


Figure 4. Record of the Pisco-Cismid earthquake.

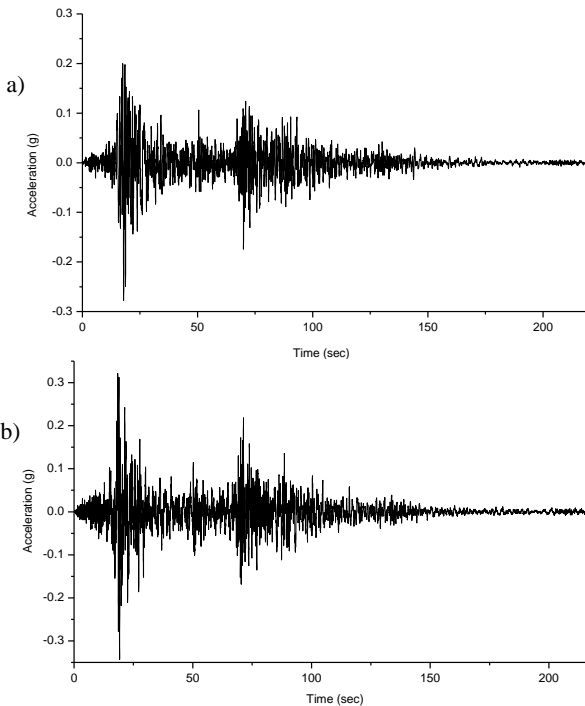


Figure 5. Record of the Moquegua-Cismid earthquake.

The design of SLB heatsinks is carried out using ETABS 18.1 software with the capacity to evaluate the nonlinearity of these heatsinks. The model has 18 devices, of which 6 heatsinks are diagonal chevron and 12 are located between walls and uncoupled beams. For its design, it is necessary to verify the level of displacement requested in each device, for which it is necessary to obtain the hysteretic time-history curve, verifying that the displacement values are less than 30 mm, which is the limit established by SLB heatsink standards, as well as the verification of the control of the demand vs. capacity by cut, /12/.

For uncoupled wall heatsinks, the stresses in connection areas are verified to provide adequate confinement. This is to absorb the tension forces generated by the rotation of the connection plate. In the case of chevron diagonals, a crenelated connection is left in the upper part, consequently, they do not transfer axial loads and only work in shear for horizontal forces, thus they will not suffer significant degradation after several load cycles, demonstrating a stable and secure connection, /8/.

## RESULTS AND DISCUSSION

As a result of analysis, in type A model, the mezzanine drifts exceed the limit proposed by the E.030-2018 standard /9/,  $0.0165 > 0.007$ , showing great flexibility of the structure in the short direction. In type B model, the interstory drifts are 0.0068.

It can be seen in Fig. 6, that with the incorporation of these devices in type B model, the damping is increased and the interstory drifts are reduced by 60 %.

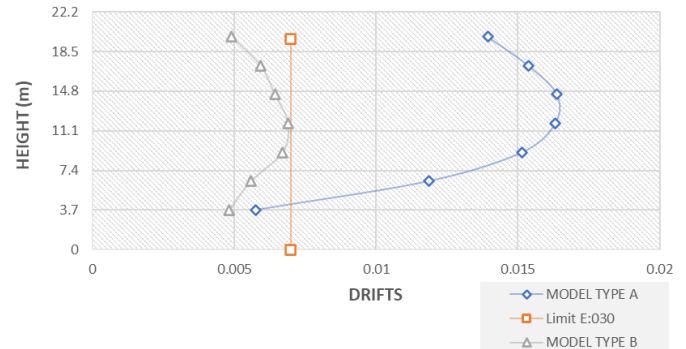


Figure 6. Drifts from measurement of types A and B models.

Table 1 shows the coefficients of torsional irregularity. For type A model are greater than for the type B model, the latter presents ratios in the short direction (X-X) less than 1.5, values that are within the range are considered acceptable for a type 4 zone in the E0.30-2018 standard.

Table 1. Coefficients of torsional irregularity.

Type A model torsion degree			
Story	Output Case	Item	Ratio
Story7	DESP X-X	Diaph D7 X	1.254
Story6	DESP X-X	Diaph D6 X	1.314
Story5	DESP X-X	Diaph D5 X	1.691
Story4	DESP X-X	Diaph D4 X	1.638
Story3	DESP X-X	Diaph D3 X	1.597
Story2	DESP X-X	Diaph D2 X	1.548
Story1	DESP X-X	Diaph D1 X	1.512
Type B model torsion degree			
Story	Output Case	Item	Ratio
Story7	DESP X-X	Diaph D7 X	1.096
Story6	DESP X-X	Diaph D6 X	1.149
Story5	DESP X-X	Diaph D5 X	1.413
Story4	DESP X-X	Diaph D4 X	1.346
Story3	DESP X-X	Diaph D3 X	1.294
Story2	DESP X-X	Diaph D2 X	1.243
Story1	DESP X-X	Diaph D1 X	1.398

It is found that the interstory displacements for type A model in the last level are  $> 25$  cm, exceeding the maximal displacement for 7 levels, which is usually approximately 1 cm per level for this type of structural system. In the type B model, reductions in lateral displacements are obtained by increasing the damping level in the structure. Figure 7 shows the different displacement values obtained, noting that the structure with SLB achieves the reduction of lateral displacements by up to 70 %.

The type A model has a maximum mezzanine acceleration of 0.65g at the last level. With type B model it is possible to obtain reductions in these accelerations of up to 20 % as shown in Fig. 8.

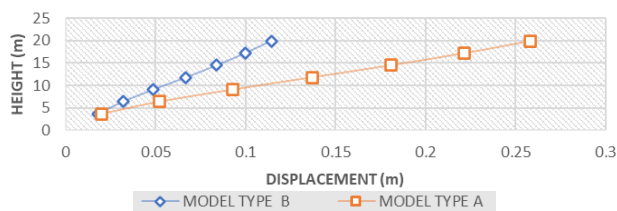


Figure 7. Maximum displacements of type A and B models.

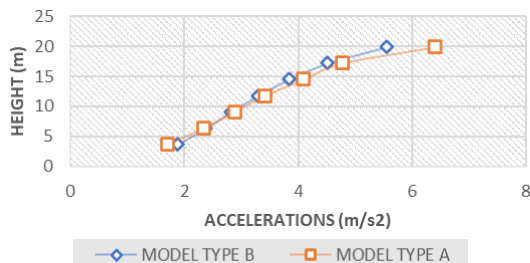


Figure 8. Floor accelerations of type A and B models.

Results of the analysis for type A model show interstory stiffness at the first level of 33685.241 tonf/m. For the type B model at the same level, it is 46398.331 tonf/m, as shown in Fig. 9 where values of lateral rigidity were increased by 40 %, qualifying as a rigid structure against lateral loads.

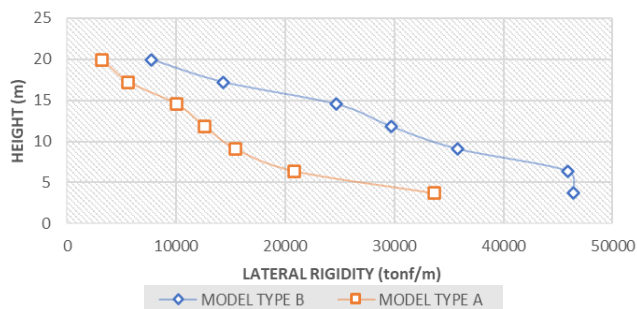


Figure 9. Maximum lateral rigidity of floor of model types A and B.

The maximum period of the structure for type A model is 0.7 s in mode 1, and 0.476 in the same mode for type B.

As part of the processing of the results obtained, the design is presented as an example of the 2 types of heatsinks used in this study.

In Fig. 10, it can be seen that the diagonal chevron located on the second level on the façade of the structure, for the Moquegua EW accelerogram, presents a demand of 552.64 kN. The maximum shear value the device supports (SLB3-25- 8) is 776.40 kN.

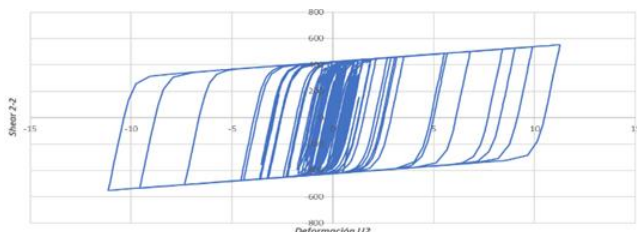


Figure 10. Hysteresis diagram- k1-thnl-axis 1-1- Moquegua EW.

In Fig. 11, the uncoupled wall located on the fifth level, for the Moquegua EW accelerogram, presents a demand of 269.13 kN, with maximum shear value supported by the device (SLB2 20-5) being 395.71 kN.

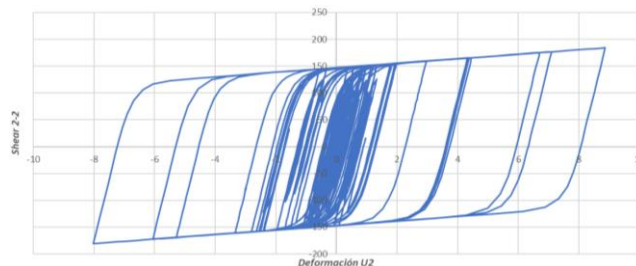


Figure 11. Hysteresis diagram- k14-thnl-axis 5-5- Moquegua EW.

Table 2 shows a summary with proposed SLB devices for the structure and their respective capacity demand.

Table 2. Heatsinks used in the type B model.

Force (kN)	Heatsink	Type	Resistance	d/c
160.42	SLB2-15-3	decoupled wall	240.45	0.66717
160.25	SLB2-15-3		240.45	0.66646
82.42	SLB2-8-4		120.87	0.68189
82.45	SLB2-8-4		120.87	0.68214
115.86	SLB2-15-4		276.57	0.41892
269.13	SLB2-20-5		395.71	0.68012
126.32	SLB2-10-5	decoupled wall	182.26	0.69308
160.94	SLB2-15-4		276.57	0.58191
127.3	SLB2-10-5		182.26	0.69845
164.46	SLB2-15-3		240.45	0.68397
124.42	SLB2-10-5		182.26	0.68265
184.23	SLB2-15-4		276.57	0.66612
128.31	SLB2-10-5	chevron	182.26	0.70399
287.21	SLB2-20-5		395.71	0.72581
552.64	SLB3-25-8		776.4	0.71180
576.36	SLB3-25-8		776.4	0.74235
496.6	SLB3-25-6		655.36	0.75775
387.75	SLB3-25-4		526.49	0.73648

## CONCLUSIONS

Results show that it is feasible to control the extreme torsion in a dual building, incorporating SLB heatsinks, estimating the location and number of these devices, in order to balance the centre of rigidity to the centre of mass of the entire structure and without the need to carry them to the base.

The use of heatsinks in flexible structures also allows to control interstory drifts, maximum displacements, and increase the lateral rigidity of the structure while reducing the seismic accelerations.

Faced with a nonlinear time-history analysis, the structures with sinks satisfactorily comply with mezzanine drifts.

These devices concentrate the ductility demands on industrially manufactured connections with defined mechanical properties, thus representing an advance to the classical design of structures based on ductility and hyperstaticity.

From the results obtained from the analysis, they show that the incorporation of SLB heatsinks to the structure and the effect they have on it, controlling extreme torsion, makes it important to include the heatsink system in the Peruvian standard E.030- 2018, considering the characteristics of Peruvian seismic records.

## REFERENCES

1. Tena-Colunga, A. (1999), *International seismic zone tabulation proposed by the 1997 UBC code: Observations for Mexico*, Earthq. Spectra, 15(2): 331-360. doi: 10.1193/1.1586044
2. Jeong, S.H., Elnashai, A.S. (2006), *New three-dimensional damage index for RC buildings with planar irregularities*, J Struct. Eng. 132(9): 1482-1490. doi: 10.1061/(ASCE)0733-9445(2006)132:9(1482)
3. Özmen, G., Girgin, K., Durgun, Y. (2014), *Torsional irregularity in multi-story structures*, Int. J Adv. Struct. Eng. 6(4): 121-131. doi: 10.1007/s40091-014-0070-5
4. Astroza, M. (2007), Study of the area affected by the Pisco earthquake, August 15, 2007. Earthquake intensities and damages. Regional Seismology Centre for South America, Mission Report CRESIS/UNESCO, Lima, Peru. (in Spanish)
5. Chianese, R.G.S. (2020), *Procedure to optimize the structural design for buildings equipped with hysteretic SLB devices*, Master's degree course in Structural and Geotechnical Eng., University of Naples Federico II, Naples, Italy. (in Italian)
6. Bozzo, L., Gonzales, H., Pantoja, M., et al. (2019), *Modeling, analysis and seismic design of structures using energy dissipators SLB*, Tecnica, 29(2): 81-90. doi: 10.21754/tecnica.v29i2.713
7. Bozzo Fernández, G. (2021), *A new generation of SLB shear link heatinks for earthquake-resistant design*, Master's thesis, Polytechnic University of Catalonia, Barcelona. (in Spanish)
8. Bozzo, L.M., Ramirez, J., Bairan, J., et al. (2020), *Precast buildings equipped with SLB seismic devices*, In: 17<sup>th</sup> World Conf. on Earthquake Engineering (17WCEE), Sendai, Japan, 2020, paper no. C001502, 12 p.
9. National Building Code, Technical Standard of Building E.030, Earthquake-Resistant Design, Lima, 2003. (last accessed Dec. 12, 2024) [https://iisee.kenken.go.jp/net/seismic\\_design\\_code/peru/NTE-030-PERU.pdf](https://iisee.kenken.go.jp/net/seismic_design_code/peru/NTE-030-PERU.pdf)
10. Tena-Colunga, A., Benítez, J.A.C. (2013), *Structural redundancy and its impact on the seismic behaviour of ductile concrete frames*, XIX National Congress of Seismic Eng., 2013, Boca del Rio, Veracruz, Mexico. Vol.: CDROM, Art. V-34, pp.1-25.
11. Observation Centre for Seismic Engineering (Dec. 2022), CISMID. <http://www.cismid.uni.edu.pe/ceois/>
12. Bozzo, L.M., et al. (2019), Procedure manual for analysis and design using SLB type seismic dissipators, Application examples, Luis Bozzo Structures and Projects S.L. (in Spanish)

© 2024 The Author. Structural Integrity and Life, Published by DIVK (The Society for Structural Integrity and Life 'Prof. Dr Stojan Sedmak') (<http://divk.inovacionicentar.rs/ivk/home.html>). This is an open access article distributed under the terms and conditions of the Creative Commons Attribution-NonCommercial-NoDerivatives 4.0 International License

## 28<sup>th</sup> International Conference on Fracture and Structural Integrity (IGF28) 3<sup>rd</sup> Mediterranean Conference on Fracture and Structural Integrity (MedFract3)

Catania (Italy) & Web, 15-18 September 2025

<https://www.igf28-medfract3.eu>

The event will be held both in person, in the beautiful setting of Aci Castello (Catania, Italy), and remotely. All remote participants will be able to participate in all sessions and discussions ... but, unfortunately, will not be able to taste the delicious food of the Sicily region!

### Topics

Analytical, computational and physical models; Biomaterials and wood fracture and fatigue; Biomechanics; Ceramics fracture and damage; Composites; Computational mechanics; Concrete & rocks; Creep fracture; Damage mechanics; Damage and fracture in materials under dynamic loading; Durability of structures; Environmentally assisted fracture; Failure analysis and case studies; Fatigue - crack growth (all materials); Fatigue resistance of metals; Fatigue of metals - very high cycle; Failure analysis and forensic engineering; Fractography and advanced metallography; Fracture and fatigue at atomistic and molecular scales; Fracture and fatigue testing systems; Fracture under mixed-mode and multiaxial loading; Fracture vs. gradient mechanics; Functional gradient materials; Impact & dynamics; Fundamentals of cohesive zone models; History of fracture mechanics and fatigue; Innovative alloys; Linear and nonlinear fracture mechanics; Materials mechanical behaviour and image analysis; Mesomechanics of fracture; Micro-mechanisms of fracture and fatigue; Multi-physics and multi-scale modelling of cracking in heterogeneous materials; Multiscale experiments and modelling; Nanostructured materials; Nondestructive examination; Physical aspects of brittle fracture; Physical aspects of ductile fracture; Polymers fracture and fatigue; Probabilistic fracture mechanics; Reliability and life extension of components; Repair and retrofitting: modelling and practical applications; Sandwiches, joints and coatings; Smart materials; Structural integrity; Temperature effect; Thin films.

### Chairpersons

Filippo Berto, Università di Roma 'Sapienza' (President)  
Sabrina Vantadori, Università di Parma (Secretary)  
Francesco Iacoviello, Università di Cassino e del Lazio Meridionale (President Emeritus)

Giuseppe Ferro, Politecnico di Torino (Vice President)  
Vittorio Di Cocco, Università di Cassino e del Lazio Meridionale (Treasurer)

### Proceedings

All the submitted papers, after being reviewed, will be published in an issue of *Procedia Structural Integrity*, the new Procedia published by Elsevier and focused on the ESIS events (indexed in Scopus, WoS and Google Scholar).

### Special issue

Authors of selected papers will be invited to submit extended versions for publication in peer reviewed special issue of *Fracture and Structural Integrity (Frattura ed integrità strutturale)*. The journal is free of charge, both for readers and for authors (no APC), and indexed (Scopus, WoS, etc).

### IGF Awards 2025

Every two years, the IGF awards up to two researchers with the following awards: Manson-Coffin IGF medal; Paolo Lazzarin IGF Medal; and IGF Award of Merit.

### Main deadlines:

Registration:	always open
Abstract submission:	Nov. 1, 2024 – May 31, 2025
Acceptance notification:	June 10, 2025
Early bird registration and payment:	July 31, 2025
Conference:	September 15-18, 2025
Paper submission:	October 15, 2025
Papers acceptance:	October 31, 2025

